Thermodynamic and transport properties of spiro-(1,1')-bipyrrolidinium tetrafluoroborate and acetonitrile mixtures: A molecular dynamics study*

Qing-Yin Zhang(张庆印)[1,†], Peng Xie(谢鹏)[1], Xin Wang(王欣)[2], Xue-Wen Yu(于学文)[3], Zhi-Qiang Shi(时志强)[3,‡], and Shi-Huai Zhao(赵世怀)[1]

[1] *The State Key Laboratory of Separation Membranes and Membrane Processes, Department of Chemical Engineering, Tianjin Polytechnic University, Tianjin* 300387, *China*

[2] *Laboratory of Chemical Engineering Thermodynamics, Department of Chemical Engineering, Tsinghua University, Beijing* 100084, *China*

[3] *Laboratory of Fiber Modification and Functional Fiber, College of Materials Science and Engineering, Tianjin Polytechnic University, Tianjin* 300387, *China*

(Received 19 October 2015; revised manuscript received 26 January 2016; published online 20 April 2016)

Organic salts such as spiro-(1,1')-bipyrrolidinium tetrafluoroborate ([SBP][BF_4]) dissolved in liquid acetonitrile (ACN) are a new kind of organic salt solution, which is expected to be used as an electrolyte in electrical double layer capacitors (EDLCs). To explore the physicochemical properties of the solution, an all-atom force field is established on the basis of AMBER parameter values and quantum mechanical calculations. Molecular dynamics (MD) simulations are carried out to explore the liquid structure and physicochemical properties of [SBP][BF_4] electrolyte at room temperature. The computed thermodynamic and transport properties match the available experimental results very well. The microscopic structures of [SBP][BF_4] salt solution are also discussed in detail. The method used in this work provides an efficient way of predicting the properties of organic salt solvent as an electrolyte in EDLCs.

Keywords: electrolyte, self-diffusion, viscosity, molecular dynamics

PACS: 61.20.Qg, 61.20.Ja, 66.20.–d, 31.15.ap **DOI:** 10.1088/1674-1056/25/6/066102

1. Introduction

The electrical double layer capacitor (EDLC), which is also frequently called super-capacitor or ultra-capacitor, is a potential electrochemical device for energy storage.[1] Because there occurs no redox reaction at the interface between the electrode and the electrolyte, the electric charge or discharge processes are entirely controlled by the Coulomb electrostatic force, and thus the EDLC shows quite a high energy density. The most important technological development for EDLC is to improve not only its power density but also its lifecycle and safety. The operational temperature, potential range and conductivity are important factors of electrolyte for further developing the EDLC. In general, the electrolytes including those based on water, ionic liquids (ILs) as well as organic salt solvents are potentially good candidates for EDLCs.[2] Although a water-based electrolyte can supply a large energy density, its operation voltage has never exceeded a value of 2.0 V.[3–5] A high-operative voltage is probably realized for the EDLC by using organic solvents. Nowadays, the EDLC is generally based on the electrolyte which is quaternary ammonium salts dissolved in organic solvent such as liquid acetonitrile (ACN) or liquid propylene carbonate (PC).[6] Although a higher operative voltage can be achieved using IL instead of organic solvent, the shortcomings of IL such as high viscosity and low conductivity should be overcome to improve the performance of IL-based EDLC under normal conditions.[7] Besides, the relatively high price of IL is another issue to prevent the IL-based EDLCs from being commercialized.[8] The above statement shows that each kind of electrolyte has its own advantages and disadvantages. Many efforts should be made to develop novel electrolytes for high-performance EDLCs in the near future.[9] Electrochemical and physicochemical properties of novel organic salt solutions or new ILs should be explored by either experiments or simulations.

Porous carbons with various pore volumes were often employed for the EDLC electrodes. In 2006, Chimola *et al.*[10] found that the capacitance of the EDLC increases abnormally when the pore size is smaller than 10 Å. Dissolution of ion in small pores might be the main reason for the anomalous enhancement of capacitance as well as energy density. The experimental work has motivated many molecular dynamics (MD) simulation investigations on the EDLCs at molecular level.[11–14] Most of the electrolytes used in simulations are ionic liquids except for those used by Yang *et al.*[11] and Feng *et al.*,[12] in which tetraethylammonium tetrafluoroborate(TEA-BF_4) salts with organic solvents were

*Project supported by the National Natural Science Foundation of China (Grant Nos. 21476172 and 51172160), the National High Technology Research and Development Program of China (Grant No. 2013AA050905), and the Natural Science Foundation of Tianjin, China (Grant Nos. 12JCZDJC28400, 14RCHZGX00859, 14JCTPJC00484, and 14JCQNJC07200).

†Corresponding author. E-mail: zhangqingyin@tjpu.edu.cn

‡Corresponding author. E-mail: shizhiqiang@tjpu.edu.cn

© 2016 Chinese Physical Society and IOP Publishing Ltd

employed as electrolytes. To the best of our knowledge, other quaternary ammonium salts have not been investigated using molecular simulations. One of the difficulties for quaternary ammonium simulation is a lack of parameters for force fields. However, developing new organic salts is an important step for the realization of EDLC and the molecular simulation technology can play an important role in understanding the mechanism of EDLC and also in designing the EDLC at molecular level. Therefore, it is necessary to develop and refine the force field for quaternary ammonium salts.

Recently, much attention has been paid to a new organic salt, the spiro-(1, 1)-bipyrrolidinium tetrafluoroborate (abbreviated as [SBP][BF_4]), due to its good electrochemical properties such as small ion size, high solubility and high conductivity.[15,16] Perricone *et al.*[17] obtained a methoxypropionitrile(MP)/ethylene carbonate(EC) mixture-based electrolyte of 1 M [SBP][BF_4]. The electrolyte presents high capacitor performance. Zheng *et al.*[18] prepared an anode of EDLC with non-porous carbon microbeads and found that the SBP cations may enlarge the storage of capability of the negative electrode. Yu *et al.*[19] and Shi *et al.*[20] synthesized [SBP][BF_4] salt and measured the electrochemical performances of [SBP][BF_4] with several organic solvents. The capacitances of the binary solvent electrolyte system could reach about 117.3 F/g at 293 K and 92.3 F/g at 323 K, respectively. The EDLC based on binary solvent system has an energy of 29.6 Wh/kg and a power density of 12.5 kW/ kg. In order to investigate the EDLC behaviors of [SBP][BF_4] organic salt electrolyte, we develop a force field for [SBP][BF_4] based on the framework of AMBER force field and density functional calculation. Then the force field is employed in MD simulations to predict the physicochemical properties of a mixture of [SBP][BF_4] and ACN. The aim of this paper is to testify to the force field of [SBP][BF_4]. In general, the simulation technique can explore the microstructure properties and dynamic properties of EDLC. An accurate force field is a prerequisite for predicting the right properties of EDLC, including electrolyte density distribution, charge distributions, orientations of ions, ionic mobilities, etc. Once the force field reproduces the right physicochemical properties of bulk electrolyte, it can be used for EDLC simulations in the future. For this purpose, we compare the simulated results with existing experimental results. Moreover the detailed microstructures of the [SBP][BF_4] and ACN mixtures are explored by molecular dynamics, which are very important for developing high-efficiency EDLCs at molecular levels.

2. Force field

In a classical molecular simulation, the accurate prediction of physicochemical properties requires a reliable and stable force field. In the present study, a twenty-five-site model for $[SBP]^+$ is adopted, and the structure of [SBP][BF_4] was calculated by density functional of Perdew, Burke and Ernzerhof[21] implemented in Dmol^3 package.[22,23] We chose the double numerical basis set with a polarization function (DNP). It was validated that the DNP basis set is comparable to 6–31 G** basis set of Gaussian basis set and Slater type orbitals, but more numerically efficient.[24,25] The geometric structure and charge distribution were calculated. Several configurations of pair ions were calculated, and the results were the same. The optimized geometries are demonstrated in Fig. 1 and the atomic charges determined by the Mulliken analysis[26,27] are given in Table 1.

The AMBER force field[28] has been successfully utilized to predict the thermodynamic properties of protein and DNA solutions[29] as well as organic compounds and ILs.[30] In this study, the AMBER force field was selected. In the AMBER force field, the potential energy E of a system can be expressed as

$$\begin{aligned} E = & \sum_{\text{bonds}} K_r(r-r_0)^2 + \sum_{\text{angles}} K_\theta(\theta-\theta_0)^2 \\ & + \sum_{\text{dihedrals}} V_n[1+\cos(n\varphi-\gamma)] \\ & + \sum_{i=1}^{N-1}\sum_{j=i+1}^{N}\left\{4\varepsilon_{ij}\left[\left(\frac{\sigma_{ij}}{r_{ij}}\right)^{12}-\left(\frac{\sigma_{ij}}{r_{ij}}\right)^{6}\right]+\frac{q_iq_j}{r_{ij}}\right\}, \end{aligned} \quad (1)$$

where r is the bond distance, θ is the bond angle, n is the dihedral multiplicity, ϕ is the dihedral angle, r_0, θ_0, γ are the equilibrium values of bond, angle, dihedral angle, K_r, K_θ, and V_n are the force constants, ε_{ij} and σ_{ij} are energy and volume parameters of Lennard-Jones (LJ) potential, r_{ij} is the distance between i and j, q_i and q_j are the charges of atom i and atom j respectively. The Lorentz–Berthelot mixing rule was applied to the LJ parameters

$$\varepsilon_{ij} = (\varepsilon_{ii}\varepsilon_{jj})^{1/2}, \quad (2)$$

$$\sigma_{ij} = \frac{\sigma_{ii}+\sigma_{jj}}{2}. \quad (3)$$

The force field parameters of [SBP][BF_4] were mainly taken from the AMBER and Andrade *et al.*[31] The model of ACN was completely cited from Ref. [32] by Wu *et al.* The charges and LJ parameters of the force field are given in Table 1, in addition, the optimized bond lengths, angles, as well as dihedrals, are also listed in Table 1.

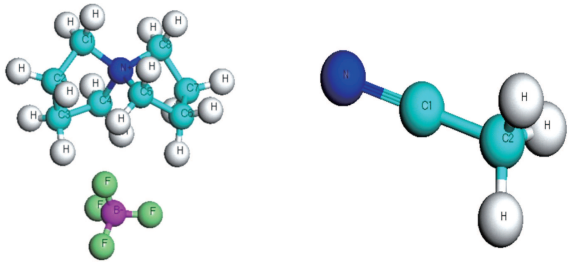


Fig. 1. (color online) Equilibrium geometries of simulated [SBP][BF_4] and ACN molecules.

Table 1. Charges and force fields for [SPB][BF_4] and ACN molecules.

Molecule	Atom	Charge[a]/e	σ_{ii}^{b}/Å	ε_{ii}^{b}/kJ·mol^{-1}	Source
SBP	C	–0.220	3.3997	0.4577	this work[a]AMBER[b]
	C	–0.056	3.3997	0.4577	this work[a] AMBER[b]
	N	–0.378	3.2500	0.7113	this work[a] AMBER[b]
	H	0.140	2.4714	0.0657	this work[a] AMBER[b]
	H	0.165	2.4714	0.0657	this work[a] AMBER[b]
BF_4	B	0.766	3.5814	0.3975	this work[a] AMBER[b]
	F	–0.431	3.1181	0.2552	this work[a] AMBER[b]
ACN	N	–0.532	3.2500	0.7113	this work[a] AMBER[b]
	C_1	0.480	3.3997	0.3598	this work[a] AMBER[b]
	C_2	–0.479	3.3997	0.4577	this work[a] AMBER[b]
	H	0.177	2.4714	0.0657	this work[a] AMBER[b]
	Bond	r_0^a/ Å	K_r^b/kJ·mol^{-1}·Å^{-2}		Source
SBP	C–C	1.55	1297.04		this work[a] AMBER[b]
	N–C	1.47	1410.01		this work[a] AMBER[b]
	C–H	1.07	1610.80		this work[a] AMBER[b]
BF_4	B–F	1.39	1213.36		Ref. [31]
ACN	N–C	1.15	2510.40		Ref. [32]
	C–C	1.46	1673.60		Ref. [32]
	C–H	1.09	1422.60		Ref. [32]
	Angle	θ_0^a/(°)	K_θ^b/kJ·mol^{-1}·rad^{-2}		Source
SBP	$N–C_{1,4,5,8}–C_{2,3,6,7}$	104.71	209.20		this work[a] AMBER[b]
	$C_{4,5}–N–C_{1,8}$	105.29	209.20		this work[a] AMBER[b]
	$C_{1,2,5,6}–C_{2,3,6,7}–C_{3,4,7,8}$	103.05	292.60		this work[a] AMBER[b]
	$C_{1,4}–N–C_{5,8}$	111.04	292.60		this work[a] AMBER[b]
	$N–C_{1,4,5,8}–H$	109.50	230.00		this work[a] AMBER[b]
	C–C–H	109.50	155.00		this work[a] AMBER[b]
	H–C–H	109.50	146.00		this work[a] AMBER[b]
BF_4	F–B–F	109.50	209.20		this work[a] AMBER[b]
ACN	$C_2–C_1–N$	180.00	334.72		Ref. [32]
	$C_1–C_2–H$	109.50	146.44		Ref. [32]
	$H–C_2–H$	109.50	127.61		this work[a] AMBER[b]
	Dihedral	V_n/kJ·mol^{-1}	n^a	γ/[a]	Source
SBP	$C_{1,5}–C_{2,6}–C_{3,7}–C_{4,8}$	0.67	3	180.0	AMBER
	$C_{2,6}–C_{3,7}–C_{4,8}–N$	0.00	1	180.0	AMBER
	$C_{2,3}–C_{1,4}–N–C_{4,1}$	0.84	2	180.0	AMBER
	$C_{3,7}–C_{4,8}–N–C_{5,1}$	0.00	1	180.0	AMBER
	H–X–X–H	0.00	2	0.0	AMBER
ACN	$N–C_1–C_2–H$	0.00	1	0.0	Ref. [32]

[a]from this work, [b]from the AMBER force field.

3. Simulation details

All-atoms molecular dynamic (MD) simulations in this work were carried out with the MD simulator LAMMPS.[33] MD simulations were first carried out at a constant temperature of 298 K and a pressure of 0.1 MPa. After equilibrium, the constant temperature and constant volume dynamics simulations were performed 10 ns for ensemble average. The Nose–Hoover thermostat was employed to control the temperature of simulating system.[34,35] The initial configurations are generated by a Monte–Carlo algorithm and ions can distribute evenly in electrolyte solution. The time-step was taken to be 1.0 fs. The ordinary three-dimensional periodic boundary conditions were used. The cutoff distance of simulated system was taken to be 15 Å. The particle–particle particle mesh (PPPM) algorithm was employed for the long-range Coulomb force calculations and the grid distance of fast Fourier transform (FFT) was 1.9 Å. The configurations of the system were saved every 100 time-steps in the simulations for further analyses. The concentrations of solution range from $x_{salt} = 0.05$ (0.9 M) to $x_{salt} = 0.142$ (2.2 M). The interval covers the working concentration range of organic salt electrolytes for realizing the EDLCs.[10,14,20] The details of the simulated systems and main simulated results of mixtures are shown in Table 2. The equilibrium configurations of the simulation box are displayed in Fig. 2.[36]

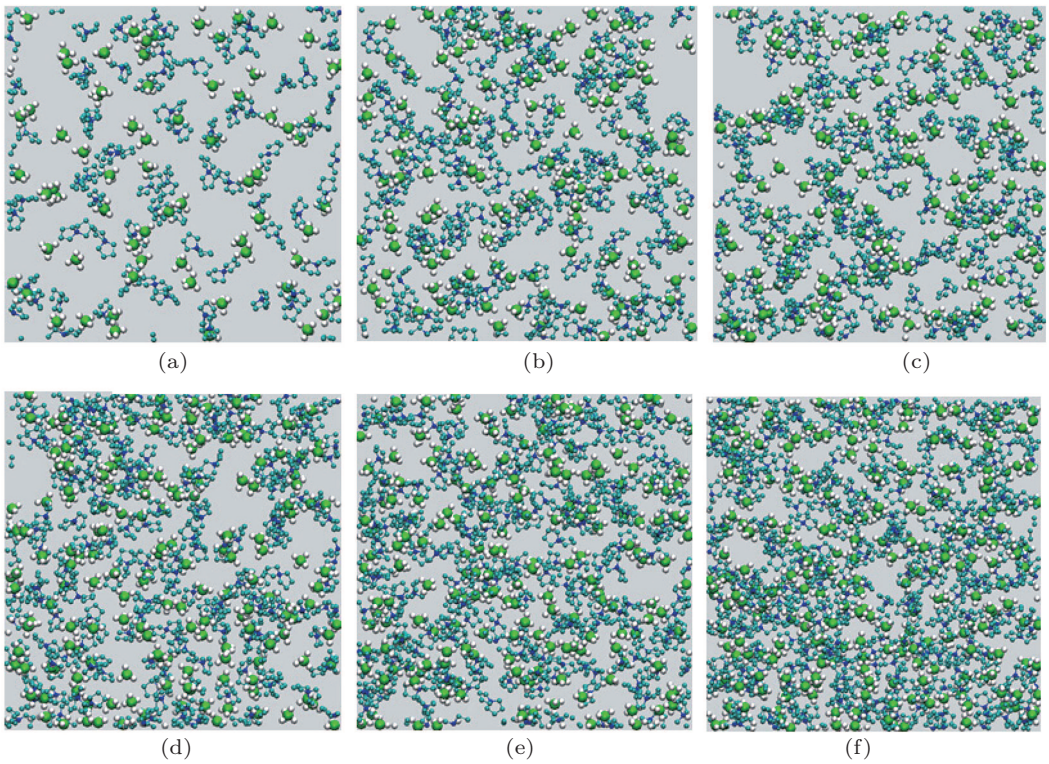


Fig. 2. (color online) Equilibrium results (the ACN and H atoms of SBP are ignored for clarity.) at $x_{salt} = 0.051$ (a), 0.090 (b), 0.101 (c), 0.119 (d), 0.130 (e), and 0.142 (f), with the colours of blue, cyan, green and white representing the atoms of N, C, B, and F*, respectively. For black–white graph, black, dark gray (big ball), light gray (small ball), and white represent the atoms of of N, C, B, and F, respectively.

Table 2. Simulation results of [SBP][BF_4] + ACN mixtures in this work.

System	Particle number		Mole fraction	Self-diffusion coefficient/10^{-11} $m^2 \cdot s^{-1}$				ρ/g·cm^{-3}	η/mPa·s	κ/S·m^{-1}
	[SBP][BF_4]	ACN	x_{salt}	D_+	D_-	D_2	D			
0	0	1331	0.000	–	–	399.4	399.4	0.781	0.52	–
1	144	2662	0.051	131.3	132.9	272.3	275.9	0.886	0.75	7.68
2	264	2662	0.090	88.7	88.1	191.4	182.1	0.975	1.14	8.60
3	150	1331	0.101	76.9	78.5	165.5	156.6	1.001	1.32	8.51
4	180	1331	0.119	59.4	58.2	117.5	110.4	1.022	1.67	7.45
5	200	1331	0.130	52.13	54.31	111.7	104.1	1.036	1.95	6.85
6	220	1331	0.142	44.0	45.6	104	96.6	1.047	2.14	6.28

In the table, D_+, D_-, D_2, D are the diffusion coefficients of cations, anions, ACN molecules and the solutions.

Table 3. Experimental results of [SBP][BF_4] + ACN mixtures in this work.

Experiment	Mole fraction x_{salt}	ρ/g·cm^{-3}	η/mPa·s	κ/S·m^{-1}
0	0	0.777	–	–
1	0.051	0.886	0.734	5.65
2	0.091	0.986	1.191	6.82
3	0.119	1.016	1.67	6.87
4	0.127	1.037	1.79	6.91
5	0.141	1.048	2.11	6.56

4. Results and discussion

4.1. Density

In MD simulations, the solid of [SBP][BF_4] was dissolved in ACN, and the densities of the mixtures are obtained for mole fraction x_{salt} in a range from 0.051 to 0.142. The simulated densities along with simulated viscosities and conductivities are given in Table 2. The values of density increase with the increase of x_{salt}. The density of the mixture at $x_{salt} = 0.142$ reaches a maximum value. In order to validate this prediction, we measured the density value of each

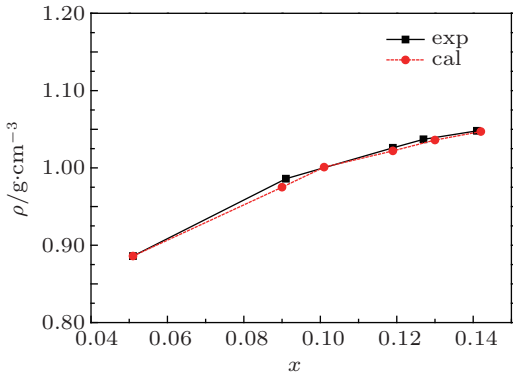


Fig. 3. (color online) Densities of the mixture [SBP][BF_4] + ACN at $T = 298$ K.

system as displayed in Fig. 3 and listed in Table 3. It should be pointed out that Table 3 also contains the experimentally measured viscosity and conductivity for the binary mixture of [SBP][BF_4]-ACN. The methods and apparatus for measuring viscosity and conductivity are the same as those in our previous work.[20] From Fig. 3, we find that the simulated densities of [SBP][BF_4] and ACN mixtures match the experimental results very well.

4.2. Microscopic structural properties of [SBP][BF_4] and ACN mixtures

Generally, distribution functions such as radial distribution functions (RDFs) are used to characterize the structure of a fluid. The RDFs have been employed to explain the microscopic structures of IL solvents.[30,37] In this work, the bulk structure of [SBP][BF_4] and ACN mixtures were studied by the site–site RDFs. The site–site RDFs for [SBP]BF_4] and ACN solvent were studied and presented in Fig. 4.

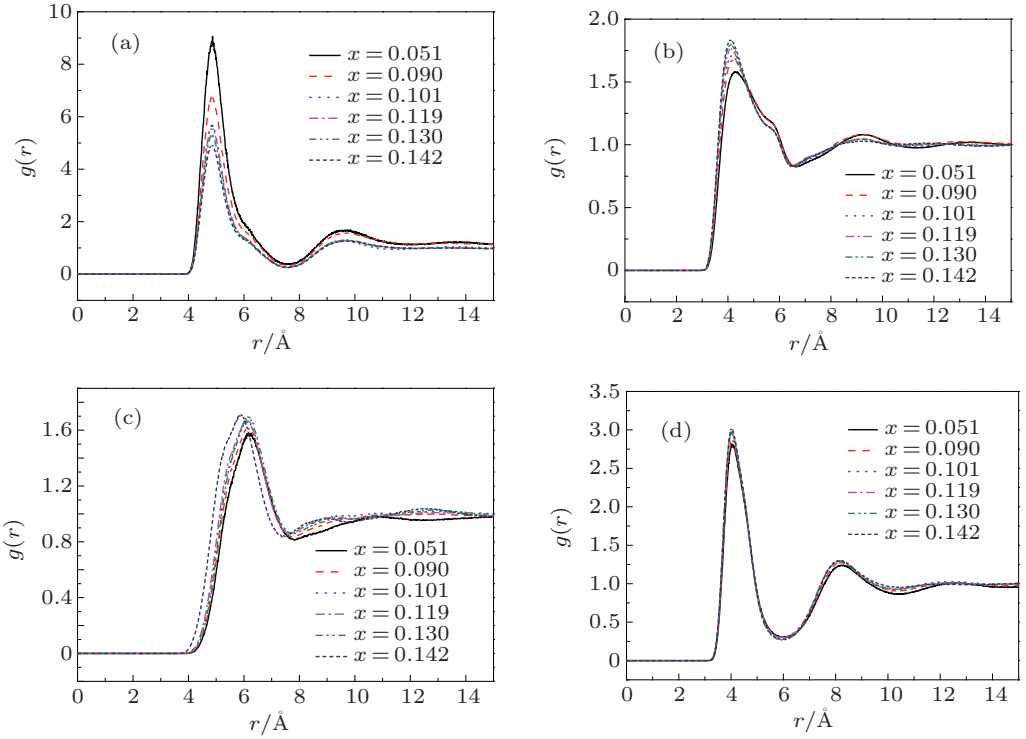


Fig. 4. (color online) (a) Cation–anion (N–B atom) RDFs, (b) C_2–C_2 atom RDFs for ACN molecule, (c) cation–ACN (N–C_2 atom) RDFs, (d) anion–ACN (B–C_2 atom) RDFs for the binary mixture of [SBP][BF_4] + ACN at $T = 298$ K. The solid, dashed, dotted, dashed-dotted, dashed dotted-dotted, and short dashed lines represent the RDFs at $x_{salt} = 0.051$, 0.090, 0.101, 0.119, 0.130 and 0.142, respectively.

The RDFs between the nitrogen atoms of the $[SBP]^+$ ions and the boron atoms of the $[BF_4]^-$ in liquid ACN are shown in Fig. 4(a). There are two main peaks in each of the RDF curves. Obviously, the positions of first peak and second peak of all concentrations are the same. The values of the first and second peaks are located at $r = 4.7$ Å and $r = 9.5$ Å respectively. The height of first peak for each curve decreases with the increase of salt concentration and the minimum value is approximately 5.1 in reduced unit when $x_{salt} = 0.142$.

Figure 4(b) shows the C_2–C_2 RDFs of an ACN molecule in the mixtures at $x_{salt} = 0.051$, 0.090, 0.101, 0.119, 0.130, and 0.142. The values of first peak at $r = 4.1$ Å increase with the increase of x_{salt}, up to a maximum for $x_{salt} = 0.142$. The positions of first peaks leftward shift slightly with the increase of x_{salt}. In the presence of [SBP][BF_4], the interactions between ACN molecules within the first layer are strengthened.

Figure 4(c) shows the N(of the cation)–C_2(of ACN molecule) atom RDFs in the mixtures. The values of first peak located at $r = 5.7$ Å increase with the increase of x_{salt}, up to a maximum for $x_{salt} = 0.142$. The position of first peak leftward shifts and the height of the peak increases with the increase of x_{salt}. The interactions between SBP cations and ACN molecules are strengthened. Because the volume of the SBP cation is large, the cation can affect the structure of solution out of the first layer. There are small second and third peaks located at 8.6 Å and 12.6 Å respectively except for the case of $x_{salt} = 0.051$. For the lowest concentration, there is only a small second peak occurring at 10.5 Å. The ultra low ion concentration may explain the abnormal RDF behaviors with other ion concentrations.

Figure 4(d) shows the B(of the anion)–C_2 (of ACN molecule) atom RDFs in the mixtures. The values of first peak located at $r = 4.1$ Å increase with the increase of x_{salt}, up to a maximum for $x_{salt} = 0.142$. The distance between the first peaks is much lower than that between cation and ACN, because the ion size of the anion is much smaller than that of the

cation. The second peaks located at $r = 8.3$ Å increase with the increase of $x_{\rm salt}$, up to a maximum for $x_{\rm salt} = 0.142$.

Through the above analyses of RDFs between $[SBP]^+$, $[BF_4]^-$, and ACN, it is concluded that interactions between cation–solvent and solvent–solvent are strengthened with the increase of the solute molecule number. The maximum peak values of RDFs between cation–ACN and the minimum peak values between cation–anion are both located at $x_{\rm salt} = 0.142$. The values of the RDFs between different peaks are related to the radius of ion or molecule. The larger the radius, the longer the distance between adjacent peaks is in the RDFs.

4.3. Mean square displacement

Ion transport of the $[SBP][BF_4]$ electrolyte can be explored in terms of the self-diffusion coefficient, which can easily be derived from the evolution of the mean square displacement (MSD) during the MD simulations according to the Einstein relationship. The MSD[38] was evaluated on the basis of the dynamic particle coordinates via

$$\mathrm{MSD} = \frac{1}{N}\left\langle \sum_{i=1}^{N} \left| \boldsymbol{r}_i^{\rm C}(t) - \boldsymbol{r}_i^{\rm C}(0) \right|^2 \right\rangle = \Delta |\boldsymbol{r}(t))|^2, \tag{4}$$

where $\boldsymbol{r}_i^{\rm C}(t)$ is the position vector of particle i, $\boldsymbol{r}_0^{\rm C}(t)$ is the initial position vector when $t = 0$, and N is the number of particles used in the simulation. The bracket denotes the statistical average of ensembles. The Einstein equation for self-diffusion is given by

$$D_i = \frac{1}{6}\lim_{t\to\infty}\frac{\mathrm{d}}{\mathrm{d}t}\left\langle \left| \boldsymbol{r}_i^{\rm C}(t) - \boldsymbol{r}_i^{\rm C}(0) \right|^2 \right\rangle, \tag{5}$$

where D_i is the self-diffusion coefficient.

In the present study, the self-diffusion coefficient for the binary mixture of $[SBP][BF_4]$–ACN was approximated by[32]

$$D = x_{\rm salt} D_{\rm salt} + x_{\rm s} D_{\rm s}, \tag{6}$$

where subscripts salt and s refer to solute $[SBP][BF_4]$ and solvent ACN respectively, and $D_{\rm salt}$ is the arithmetic average of D_+ and D_-.

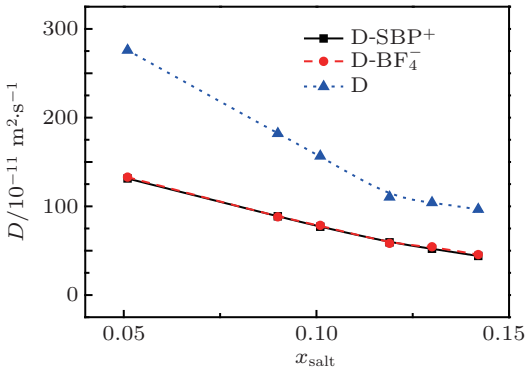


Fig. 5. (color online) Variations of self-diffusion coefficient with mole fraction $x_{\rm salt}$ for $[SBP]^+$, $[BF_4]^-$ and ACN at $T = 298$ K.

The predicted self-diffusion coefficients for cations, anions, ACN and solution are illustrated in Fig. 5. The simulated values of self-diffusion coefficients along with simulated densities, viscosities and conductivities are listed in Table 2. The self-diffusion coefficients are calculated by the slopes of the linear region of MSD curves. It is noticed that the self-diffusion coefficient of pure ACN obtained in the present study is 3.994×10^{-9} m^2·s^{-1}, which is very close to the simulation value (3.927×10^{-9} m^2·s^{-1}) replotted by Wu *et al.*[32] As demonstrated in Fig. 5, the simulated self-diffusion coefficient decreases monotonically as $x_{\rm salt}$ is increased in all the cases.

4.4. Kinematic viscosity and electro-conductivity

Figure 6 shows the comparisons between computed and experimental viscosities for $[SBP][BF_4]$ and ACN mixtures. The viscosities can be estimated from the Stokes–Einstein relation,[39,40] and if one assumes that the Stokes–Einstein relation can be applied to this organic salt electrolytes system, then the viscosity for the solution can be estimated from the following relation[41]

$$\eta_{\rm IL} = \eta_{\rm H_2O}\frac{D_{\rm H_2O}}{D_{\rm IL}}. \tag{7}$$

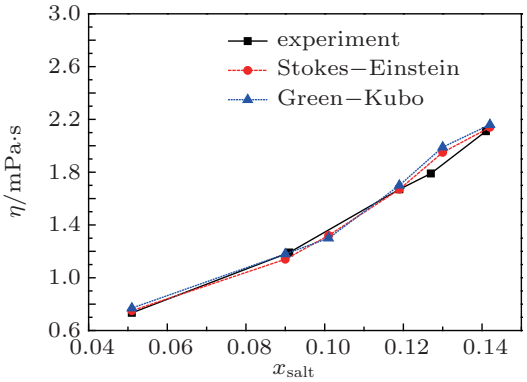


Fig. 6. (color online) Variations of viscosity with mole fraction $x_{\rm salt}$ for the mixture $[SBP][BF_4]$ and ACN at $T = 298$ K. The solid, dashed and dotted lines represent the experimental values, calculated values from Stokes–Einstein equation and Green–Kubo equation respectively.

The self-diffusion coefficient of water at 298 K and 0.1 MPa is 2.3×10^{-9} m^2·s^{-1}, and $\eta_{\rm H_2O} = 0.9$ mPa·s. As a result, one can calculate the viscosity from Eq. (7) using simulated self-diffusion coefficient. The estimated viscosity obtained using this method can be found in Table 2. Except for Eq. (7), the viscosity values of electrolytes can be calculated by the Green–Kubo equation. The Green–Kubo equation for viscosity[42] is given as follows:

$$\eta = \frac{V}{k_{\rm B}T}\int_0^\infty \left\langle P_{\alpha\beta}(t)\cdot P_{\alpha\beta}(0)\right\rangle \mathrm{d}t, \tag{8}$$

$$P_{\alpha\beta}(t) = \frac{1}{V}\left[\sum_i m_i \cdot v_{i\alpha}(t)\cdot v_{i\beta}(t) + \sum_i r_{i\alpha}(t)\cdot f_{i\beta}(t)\right], \tag{9}$$

where $\alpha\beta = xy$, xz, yx, yz, zx, or zy; $P_{\alpha\beta}$ is the $\alpha\beta$ component of the molecular stress tensor$P$ of the system; V is the volume of system; $k_{\rm B}$ is the Boltzmann constant.

At the same time, we also measured the viscosities and electro-conductivities. These experimental results are included in Table 3. As shown in Fig. 6, the calculated results

based on Eq. (7) or the Green–Kubo equation are close to the experimental results. The values of viscosity increase with the increase of the solute, while the influence of volume of [SBP][BF_4] molecule on the viscosity appears at $x_{salt} = 0.142$.

The Nernst–Einstein equation[43] can be used to evaluate the conductivity (κ) via

$$\kappa = \frac{N_{ion} q^2 (D_+ + D_-)}{k_B T}, \tag{10}$$

where q is the charge on each particle and N_{ion} is the number of ions per unit volume. The electro-conductivity can be derived according to Eq. (10) from the simulated diffusion coefficient for the binary mixture of [SBP][BF_4]–ACN. The derived results are shown in Fig. 7 and Table 2. The calculated conductivity values between $x_{salt} = 0.12$ and $x_{salt} = 0.14$ are close to the experimental data. The conductivity values at low concentrations are higher than those of experimental results. At low concentrations, the freedoms of ions are large and the migrations of ions are quite fast. All the movements of particles are attributed to diffusions, and the solution molecule can also disturb the mobility of ions. However, the experimental conductivities presented here are determined directly by impedance method, only the mobility of ions is taken into account. As discussed by Perricone *et al.*,[17] the Nernst–Einstein equation might overestimate the value of conductivity at low concentration. Though there are some deviations of simulation result from experimental result, the simulation can predict the variation trend of conductivities for [SBP][BF_4] electrolytes.

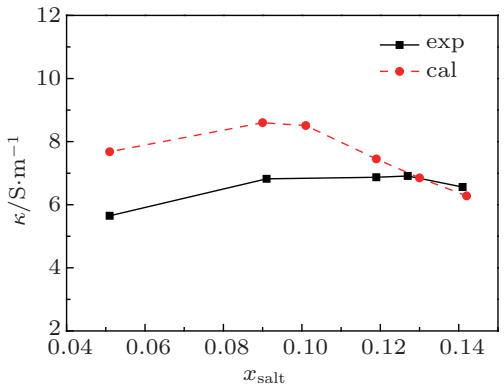


Fig. 7. (color online) Variations of measured and calculated conductivity with mole fraction x_{salt} for the mixture [SBP][BF_4] and ACN at $T = 298$ K.

5. Conclusions

The development of electrical double layer capacitors requires an in depth understanding of the interactions between the molecules. Molecular simulations provide a powerful tool at molecular level to meet this requirement for EDLC development. In this work, a force field for an organic salt solution is developed and the MD simulations are performed to predict the densities, self-diffusion coefficients, viscosities, and conductivities of [SBP][BF_4] + ACN binary solution under different conditions. The MD simulations reproduce the densities for the binary mixture of [SBP][BF_4] + ACN very well. Based on the self-diffusion coefficients sampled from the trajectories of simulated systems, the viscosities of the mixtures are predicted by the Stokes–Einstein equation, which match the experimental results well. Through RDF analysis, the interactions of cation–solvent and solvent–solvent become stronger with the increase of concentration. In addition, as the mole fraction x_{salt} is increased, the change tendency of conductivity of mixtures is in agreement with that from the experiment.

In summary, based on the framework of AMBER and quantum mechanics calculations, the force field is developed in the present study and has been successfully applied to the binary mixtures of [SBP][BF_4] and ACN. The predicted properties agree well with the corresponding experimental data. The EDLCs have higher power density than rechargeable batteries in that the electrical charge is stored in the electrical double layer formed at the electrode/electrolyte interface, which could rapidly adsorb–desorb without faradic reactions. So, the electrolytes used in EDLCs demand high electrical conductivity and low viscosity to enable the high mobilities of the electrolyte ions between the two electrodes. In other words, the electrolytes with low electrical conductivity and high viscosity supply low mobility and high electrolyte solution resistance, which is improperly used in high-power performance application. For realizing the EDLCs, new electrolytes, which have high conductivities and low viscosities, should be developed and tested. To choose and testify the electrolytes requires a large amount of experimental work. With the help of molecular dynamics simulation, based on the force field developing method presented here, it is easy to predict the viscosities and conductivities of a novel electrolyte under different conditions. Simulations will reduce the experimental jobs and save time in developing electrolytes. In conclusion, this work provides a good way to understand and estimate the macroscopic properties of the organic salt solutions that have promise to be used in the electrical double layer capacitors.

References

[1] Kotz R and Carlen M 2000 *Electrochim. Acta* **45** 2483
[2] Hall P J, Mirzaeian M, Fletcher S I, Sillars F B, Rennie A J R, Shitta-Bey G O, Wilson G, Cruden A and Carter R 2010 *Energy Environ. Sci.* **3** 1238
[3] Gao Q, Demarconnay L, Raymundo-Pinero E and Beguin F 2012 *Energy Environ. Sci.* **5** 9611
[4] Demarconnay L, Raymundo-Pinero E and Beguin F 2010 *Electrochem. Commun.* **12** 1275
[5] Fic K, Lota G, Meller M and Frackowiak E 2012 *Energy Environ. Sci.* **5** 5842
[6] Burke A 2007 *Electrochim. Acta* **53** 1083
[7] Beguin F, Presser V, Balducci A and Frackowiak E 2014 *Adv. Mater.* **26** 2219
[8] Plechkova N V and Seddon K R 2008 *Chem. Soc. Rev.* **37** 123
[9] Schuetter C, Husch T, Korth M and Balducci A 2015 *J. Phys. Chem. C* **119** 13413
[10] Chmiola J, Yushin G, Gogotsi Y, Portet C, Simon P and Taberna P L 2006 *Science* **313** 1760
[11] Yang L, Fishbine B H, Migliori A and Pratt L R 2009 *J. Am. Chem. Soc.* **131** 12373

[12] Feng G, Huang J, Sumpter B G, Meunier V and Qiao R 2010 *Phys. Chem. Chem. Phys.* **12** 5468
[13] Vatamanu J, Borodin O and Smith G D 2011 *J. Phys. Chem. B* **115** 3073
[14] Shim Y, Jung Y and Kim H J 2011 *J. Phys. Chem. C* **115** 23574
[15] Higashiya S, Devarajan T S, Rane-Fondacaro M V, Dangler C, Snyder J and Haldar P 2009 *Helv. Chim. Acta* **92** 1600
[16] Chiba K, Ueda T and Yamamoto H 2007 *Electrochem.* **75** 664
[17] Perricone E, Chamas M, Lepretre J C, Judeinstein P, Azais P, Raymundo-Pinero E, Beguin F and Alloin F 2013 *J. Power Sources* **239** 217
[18] Zheng C, Gao J, Yoshio M, Qi L and Wang H 2013 *J. Power Sources* **231** 29
[19] Yu X, Ruan D, Wu C, Wang J and Shi Z 2014 *J. Power Sources* **265** 309
[20] Shi Z, Yu X, Wang J, Hu H and Wu C 2015 *Electrochim. Acta* **174** 215
[21] Perdew J P, Burke K and Ernzerhof M 1996 *Phys. Rev. Lett.* **77** 3865
[22] Delley B 1996 *J. Phys. Chem.* **100** 6107
[23] Delley B 2000 *J. Chem. Phys.* **113** 7756
[24] Yu Y X 2013 *J. Mater. Chem. A* **1** 13559
[25] Yu Y X 2014 *ACS Appl. Mater. Interfaces* **6** 16267
[26] Mulliken R S 1955 *J. Chem. Phys.* **23** 1833
[27] Yu Y X 2013 *Phys. Chem. Chem. Phys.* **15** 16819
[28] Weiner S J, Kollman P A, Case D A, Singh U C, Ghio C, Alagona G, Profeta S and Weiner P 1984 *J. Am. Chem. Soc.* **106** 765
[29] Yu Y X and Fujinoto S 2013 *Sci. China: Chem.* **56** 1735
[30] Soolo E, Brandell D, Liivat A, Kasemagi H, Tamm T and Aabloo A 2012 *J. Mol. Model.* **18** 1541
[31] De Andrade J, Boes E S and Stassen H 2002 *J. Phys. Chem. B* **106** 13344
[32] Wu X, Liu Z, Huang S and Wang W 2005 *Phys. Chem. Chem. Phys.* **7** 2771
[33] Plimpton S 1995 *J. Comput. Phys.* **117** 1
[34] Nose S 1984 *J. Chem. Phys.* **81** 511
[35] Hoover W G 1985 *Phys. Rev. A* **31** 1695
[36] Humphrey W, Dalke A and Schulten K 1996 *J. Molec. Graphics* **14** 33
[37] Zeng J, Zhang Y, Sun R and Chen S 2014 *Electrochim. Acta* **134** 193
[38] Fan Y S, Chen X, Zhou W, Shi S P and Li Y 2011 *Acta Phys. Sin.* **60** 032802 (in Chinese)
[39] Farhadian N and Malek K 2014 *Solid State Ionics* **268** 162
[40] Ju Y Y, Zhang Q M, Gong Z Z and Ji G F 2013 *Chin. Phys. B* **22** 083101
[41] Morrow T I and Maginn E J 2003 *J. Phys. Chem. B* **106** 12807
[42] Allen M P and Tildesley D J 1987 *Computer Simulation of Liquids* (Oxford: Clarendon Press) pp. 64–64
[43] Noda A, Hayamizu K and Watanabe M 2001 *J. Phys. Chem. B* **105** 4603